STUDIES AND RESEARCHES – V. 27, 2007
Graduate School in Concrete Structures – Fratelli Pesenti
Politecnico di Milano, Italy

A RE-EVALUATION OF TEST RESULTS ON BOND IN R/C BY MEANS OF FE MODELING

(Final text, September 2007)

Miguel Fernández Ruiz[1], Aurelio Muttoni[2] and Pietro G. Gambarova[3]

ABSTRACT

The role of various parameters governing bond behavior is investigated in this paper taking advantage of a simple but efficient finite-element model, whose fundamental aspects are briefly recalled. Several well-documented test results on bond are examined in order to clarify the relevance of some aspects of bond phenomenological behavior, and to study a few bond situations where testing has been scarce in the past, as in the case of push-in tests. Parametric studies are performed as well, with reference to the loading mode (pull-out and push-in), to bar elastic and strain-hardening moduli, to steel yield strength and to bar lateral contraction/expansion, both in the elastic and in the plastic domain. Beside contributing to a better understanding of the role of the above-mentioned parameters, the paper confirms at the same time the uniqueness of the local bond stress-slip law, and the necessity of introducing a corrective factor, in order to take care of the damage to bond caused by the cone-shaped microcracks radiating from the bar close to the transverse cracks in tension ties and to the flexural cracks in R/C beams subjected to bending.

---

[1] Post-Doctoral Fellow, Ecole Polytechnique Fédérale de Lausanne, IS-BETON, Lausanne, Switzerland.
[2] Professor, Ecole Polytechnique Fédérale de Lausanne, IS-BETON, Lausanne, Switzerland.
[3] Professor, Politecnico di Milano, Dept. of Structural Engineering, Milan, Italy, on leave at EPFL in Spring 2006.

1. INTRODUCTION

Bond governs many phenomena in structural concrete, from first loading (cracking, tension–stiffening) to failure (structural ductility). Bond is activated under various actions (pure tension, pull–out, push–in ...) and depends on many geometrical parameters (short/long embedment-length, small/large concrete cover, small/large bar diameter ...), and on the physical properties of both the reinforcing bars (elastic and hardening moduli, yield strength ...) and the concrete (compressive strength, confinement level ...).

In this paper, a finite-element model is used with the aim of investigating bond mechanics and thus the role of the aforementioned parameters. Several available test results are analyzed and the phenomena governing bond are explained on the basis of the numerical simulations. The FE model is also used (a) to perform several parametric studies for values of the parameters other than those concerning the tests, and (b) to perform a few numerical tests in a number of cases where test results are scanty or even unavailable. The following topics are investigated in this paper:

1. Local bond law in long anchored bars.
2. Role of the lateral expansion/contraction of a reinforcing bar and of its longitudinal strain (both in the elastic and plastic domains) on bond behavior.
3. Role of the yield strength and hardening modulus on the post–yield response of bond.
4. Effect that the development of conical microcracks (close to the flexural cracks of a member in bending or to the end sections of a tension tie) has on the bond–stress distribution.

The numerical results, together with the physical interpretations given in the paper, provide further justification of:

- the affinity hypothesis of the bond–slip curves for long anchored bars (Fernández Ruiz et al., 2007);
- the local bond-strength reduction close to the end sections of a tension tie; and
- the role of the bond coefficient introduced by the authors in a previous work (Fernández Ruiz et al., 2007).

2. FINITE-ELEMENT MODEL

The choice of the finite-element method for bond modeling allows to consider several coupled phenomena (plasticity, contact, cracking ...). This is the reason why FEM has been applied to bond modeling by several researchers, from the pioneer work of Ngo and Scordelis (1967) to the most recent advancements (Lundgren, 2001; Salem and Maekawa, 2004; Bamonte et al., 2003; Bamonte and

Gambarova, 2007; an extended synthesis of the previous work on bond and on the ongoing developments can be found in FIB Bulletin No.10, 2000). In this paper a simple but efficient finite-element model (implemented into the FE code ANSYS, from ANSYS Inc.) is used to investigate some phenomenological aspects concerning bond. Some details of the finite-element model are shown in Fig.1.

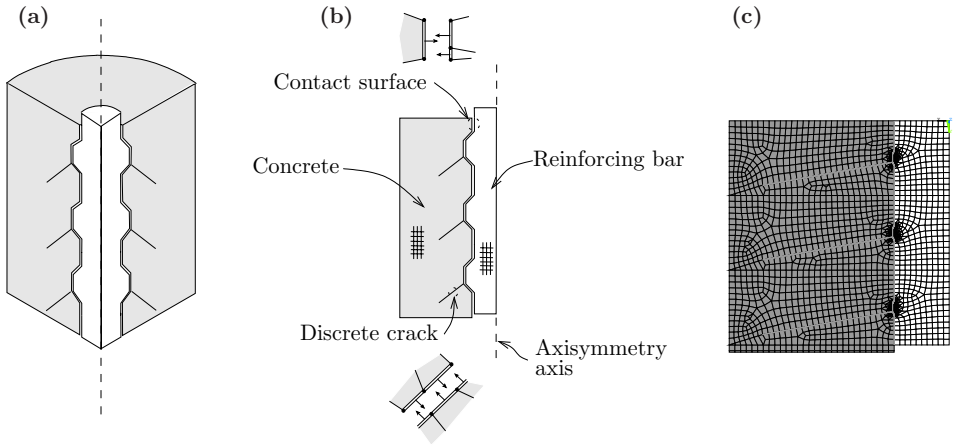

Fig. 1 - Finite-element model: (a) one quarter of the axi-symmetric specimen; (b) outline of the axi-symmetric model and of the contact elements; and (c) details of the mesh.

The bond problem is described by means of an axial-symmetric bi–dimensional model with finite deformations. For the ribs, an equivalent geometry with the same bond index (i_R) as in the actual ribs is adopted in order to simplify the numerical problem (i_R usually ranges between 0.05 and 0.10). The concrete and the reinforcing bar have been modeled by using eight–node elements with compatible displacement shapes and 2×2 integration points.

The reinforcing steel is assumed to have an elastic–plastic behavior controlled by Von Mises' yield criterion and with strain hardening. For the concrete, an elastic–plastic constitutive law has been adopted, but discrete cracking is introduced as well. Under compression, the stresses are moderate (far below the crushing strength of the material) except in the zones closest to the ribs, where concrete is highly confined and exhibits a ductile post–yield response with strain hardening (Schenkel, 1998). In order to describe this behavior, the Von Mises' yield criterion with strain hardening has been adopted even if other criteria (for instance Drucker–Prager's criterion) are in principle more suitable for concrete in compression. Both criteria are compared in Fig.2, where according to Von Mises' criterion the cylinder representing the yield surface expands, as the material hardens with increasing plastic strains.

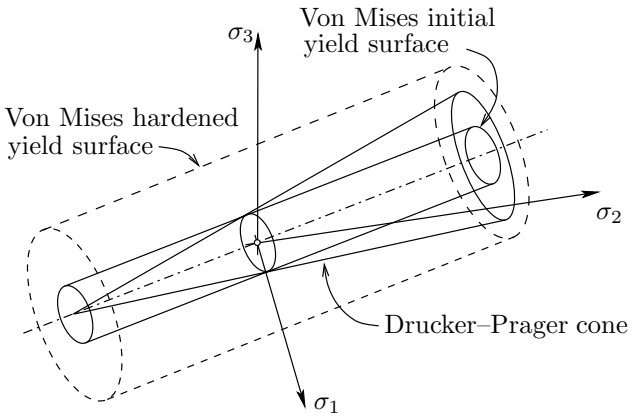

Fig. 2 - Concrete yield surface: Von Mises' yield criterion with strain hardening and Drucker–Prager's criterion.

Although the response of concrete is reasonably well reproduced in compression with Von Mises' criterion, unrealistic stresses are obtained in tension. In the actual bond conditions, the tensile stresses are moderate (and acceptable) except close to the ribs, where high tensile stresses develop at an angle between 45° and 80° with respect to bar axis. In order to avoid such large stresses, inclined discrete cracks have been introduced (Fig.1), where the optimal crack orientation has been identified by performing an elastic (uncracked) analysis of the system.

As for the interface between the bar and the concrete, surface–to–surface contact elements formulated with an augmented Lagrange multiplier have been defined. These elements have 3 nodes (since the underlying solid elements have mid-side nodes) with two integration points. The friction coefficient at the steel–concrete interface has been given the value 0.30. No cohesion has been considered at the interface. Similar contact elements are introduced along the inclined cracks, to guarantee that compression stresses can be transmitted across the closed part of each crack.

Two solvers were tested, a full Newton–Raphson and an un-symmetric full Newton–Raphson (because of the contact elements). Finally, the un-symmetric solver was adopted, because of its better performance.

Although the model has certain limitations, its behavior is reasonably accurate in the various cases examined in the following, and a good agreement with the experimental data has been found.

3. PULL–OUT TESTS

Pull–out tests on short anchored bars ($L/\phi_s \leq 5$, Fig.3) are generally performed to determine the local bond stress–slip law ($\tau_s(\delta)$). In these specimens (be they

cylinders or cubes), the slip is approximately constant along the bonded length L of the bar and the bond stress is roughly uniform : $\tau_s(\delta) = F/(\pi \cdot \phi_s \cdot L)$. Concrete strength and rib geometry are the key parameters controlling bar response.

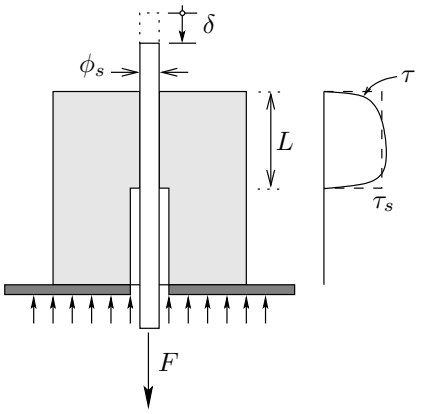

Fig. 3 - Setup of the pull–out tests on short anchored bars: τ_s = mean bond stress, and τ = local bond stress; in short anchored bars $\tau \cong \tau_s$ $(L/\phi_s \leq 5)$.

In long anchored bars, however, the pull–out response is different since bond failure is preceded by bar yielding (if enough concrete cover and/or confinement are provided) and the relative steel–concrete slip is no longer constant along the bonded length. As a result, bond is not only influenced by the relative slip, but also by the variable strain in the bar (Shima et al. 1987a, 1987b; Bigaj 1999). In the following, the FEM results are used to investigate bond mechanics of long pull–out specimens, as well as to assess the influence that the strain in the bar has on the local bond response.

3.1 Tests by Shima et al.

Shima et al. (1987a) performed several pull–out tests on long specimens to study the effect that bar yielding has on bond behavior (Fig.4a). As shown in Fig.4b, the numerical results fit rather well the test results (specimen SD–70), both before and after bar yielding, though the extent of the plasticized zone predicted by FE analysis is smaller than that measured by Shima. In Fig.4c the plots of τ versus δ and ε_s are shown for all sections of the bar and for all load steps. It is interesting to note that a unique relationship is found between δ and ε_s (and consequently between τ and ε_s) for any load step. This result confirms the hypothesis of affinity proposed by Fernández Ruiz et al. (2007) that allows a simple analytical treatment of bond problems.

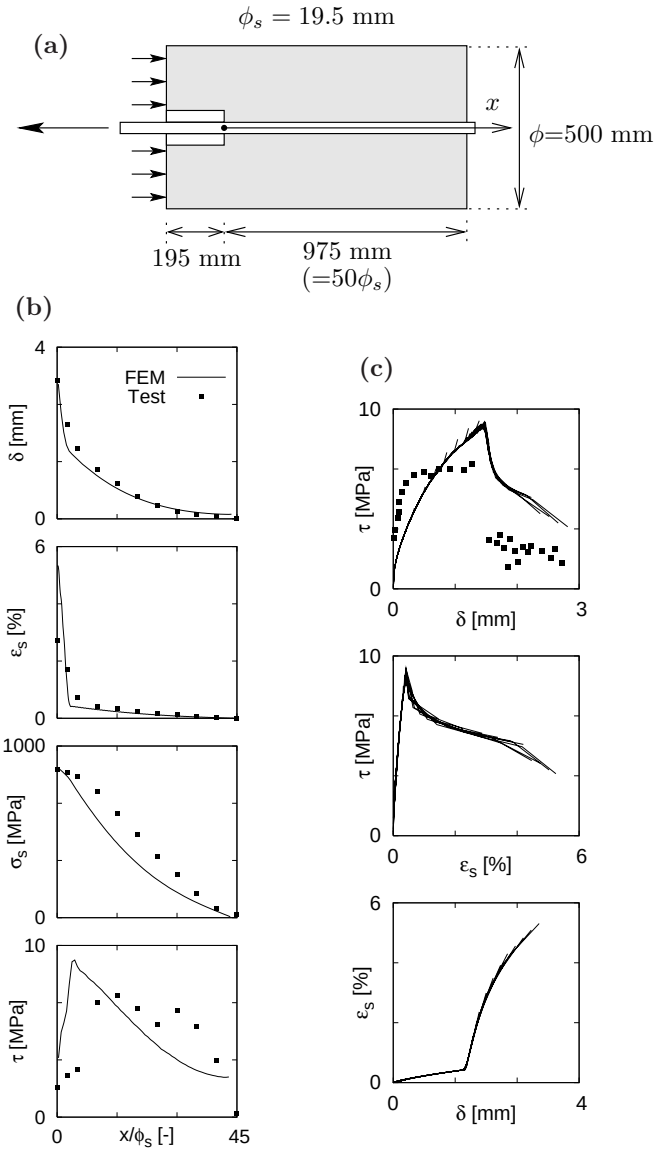

Fig. 4 - Test SD–70 by Shima et al. (1987a): (a) test set–up (f_c = 19 MPa, f_y = 820 MPa, E_s = 190 GPa and E_h = 2 GPa); (b) experimental and FEM results along the axis of the bar after yielding for P/P_{yield} = 1.05; and (c) various diagrams (bond stress versus bar slip and bar strain, and bar strain versus bar slip) for all load steps and bar sections.

FEM results also confirm the uniqueness of the bond law $\tau(\delta)$, that is independent of the load step and of the position of the rib, as shown also in Fig.5c, where the values of τ versus δ are aligned along the same curve for all the sections of the bar ($0 \le x \le L$), at the onset of yielding (a) and at the last load step (b).

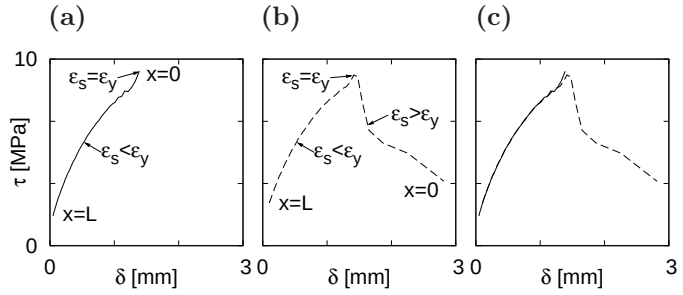

Fig. 5 - Test SD–70 by Shima et al. (1987a): (a) numerical results at the onset of bar yielding ($P/P_{yield} = 1$); (b) results at the last load step ($P/P_{yield} = 1.05$); and (c) superposition of both cases.

3.2 Tests by Bigaj

Bigaj (1995) performed several tests on the post–yield behavior of long anchored bars. A comparison between the experimental results and those obtained with FEM is presented in Fig.6, where again the agreement is good and the development of the plasticized zone is properly described.

4. PUSH–IN TESTS

In push–in tests, the bar is not pulled out from one end but is pushed into the concrete from the other. Again, short and long embedment lengths exhibit different behaviors. In short anchored bars, the behavior is similar to that of pull–out tests. The bar slip is constant and bond is controlled by concrete strength and rib geometry.

In long specimens, the response is affected by the strains in the bar. Unfortunately, no experimental results have been found on this topic, though some theoretical works have been performed (see for instance Russo and Romano, 1991). For such reasons, the layout of the specimen SD–70 tested by Shima in the pull–out mode has been used in order to reproduce a push–in test and to make comparisons (Fig.7).

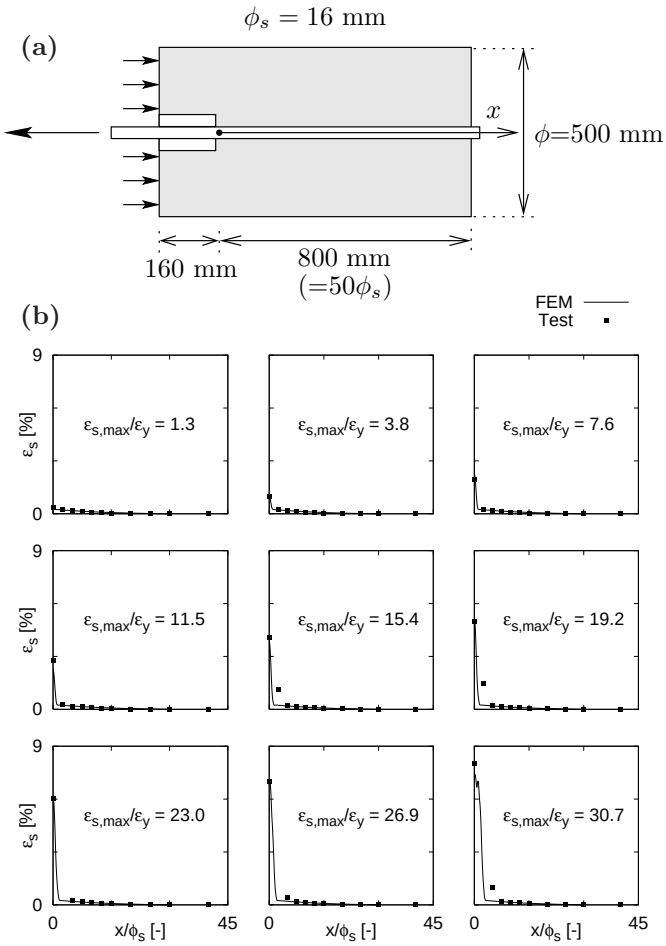

Fig. 6 - Test 16.16.1 by Bigaj (1995, f_c = 27 MPa, f_y = 540 MPa, E_s = 210 GPa and E_h = 0.8 GPa): (a) test set–up; and (b) comparison with FEM results at different load steps.

Figure 7 shows the results obtained when the bar is pushed into the concrete from the opposite end with respect to the reaction plate. It is interesting to note that - contrary to pull–out tests - the bond stress increases once the bar yields (Fig.7c). This fact can be explained by the lateral expansion of the bar in compression that improves the wedging effect of the bar (known as Hoyer's effect), contrary to the lateral contraction of the bar in pull–out tests (that reduces bond stress as previously shown in Fig.4c). This mechanism of lateral expansion/contraction is thus identified as a main phenomenon governing bond strength.

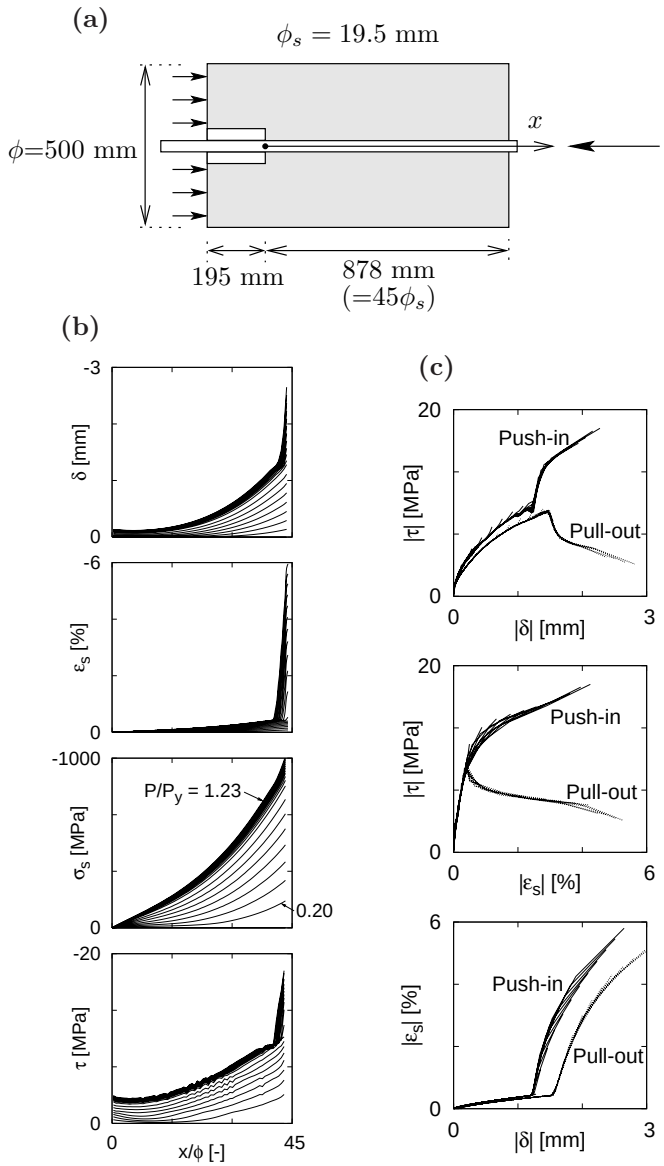

Fig. 7 - Numerical tests in the push–in and pull-out modes: (a) assumed test set–up (very close to Test SD-70 by Shima et al., 1987a); (b) FEM results along the axis of the bar at different load steps; and (c) various diagrams (bond stress versus bar slip and bar strain, and bar strain versus bar slip) for all load steps and bar sections.

5. PARAMETRIC STUDY OF LONG PULL–OUT TESTS

This section studies the influence of various parameters in bond response, in order to explain their relevance to bond mechanics and their physical role.

5.1 Elastic modulus

The influence of the elastic modulus in the response of a bar was studied by Shima et al. (1987c), who performed some pull-out tests with steel bars (E_s = 190 GPa) and with aluminium bars (E_s = 70 GPa). Figure 8 presents a comparison between the test results and FEM analysis. Note that in Fig.8 the elastic modulus of the bar is always indicated with E_s, but E_s = 190 GPa stands for "steel" and E_s = 70 GPa stands for "aluminium". The values E_s = 10 and 10000 GPa represent two limit cases (very soft material the former case and very stiff material the latter case). Furthermore, Figure 8b shows that the larger the stiffness of the bar, the more constant the slip, since the bar tends to behave like a rigid body and the long–bar behavior tends to coincide with the short-bar behavior.

As for the fitting of the test results by Shima et al. (1987c), Fig.8d shows that the agreement is rather satisfactory for low-modulus bars (aluminium bars with E_s = 70 GPa), but unsatisfactory for high-modulus bars (steel bars with E_s = 190 GPa). The trend, however, is suitably reproduced.

5.2 Hardening modulus

The hardening modulus of a reinforcing bar (E_h) is one of the main parameters controlling the post–yield response of bond. Figure 9 shows the results obtained for the geometry and properties of specimen SD–70 (Shima et al. 1987a) by means of FEM analysis, for different values of E_h (= 0-0.25·E_s = 0-50 GPa). It can be observed that the plasticized zone becomes smaller and a greater decrease in the post–yield bond stresses occurs when smaller values of the hardening modulus are considered.

This result is very reasonable, since for a given increase of the strains in the plasticized zone, the difference in terms of longitudinal stresses (that have to be transmitted by bond) is smaller as the hardening modulus decreases. In any case, one should note that the yielding of the material develops gradually, leading to a gradual decrease of the bond stresses.

5.3 Yield strength

The influence of the yield strength in the post–yield response of bond was also studied by Shima et al. (1987c). The results of three specimens tested by Shima with three different yield strengths for the bars (f_y = 350, 610 and 820 MPa) are considered. FEM results are compared with the experimental measurements in Fig.

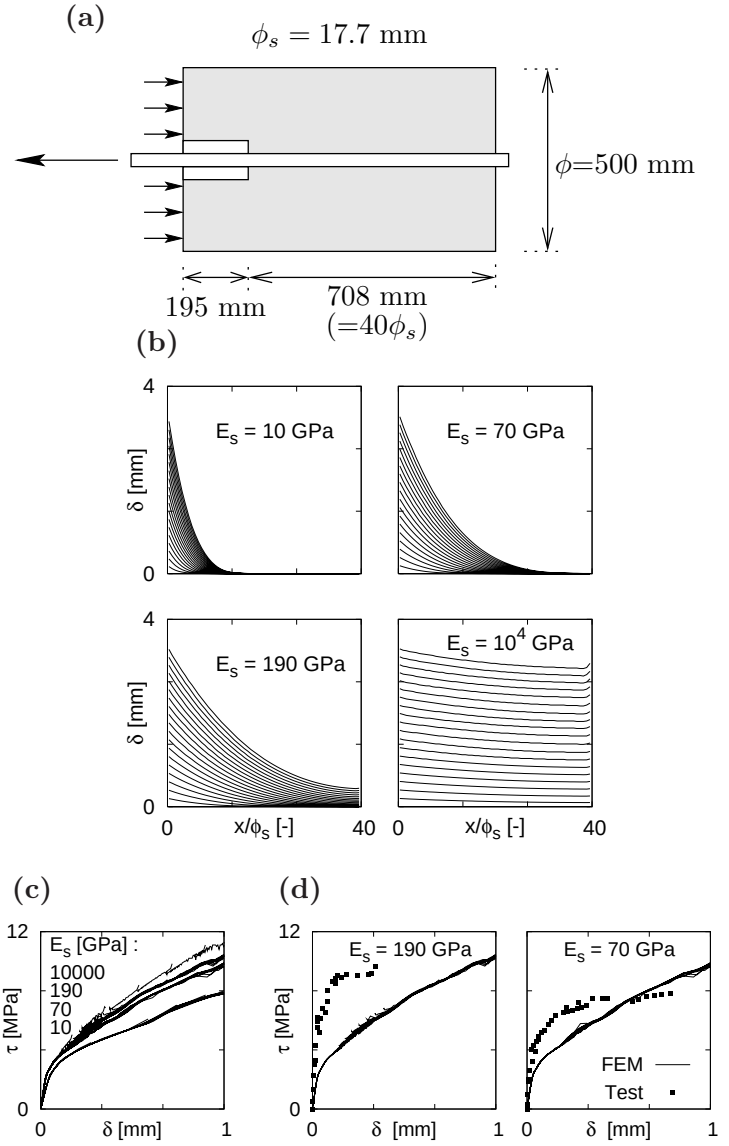

Fig. 8 - Influence of the elastic modulus on bond response: (a) pull–out tests by Shima et al. (1987c) on steel and aluminium bars; (b) FEM results concerning the relative steel–concrete slip for different values of the elastic modulus; (c) FEM results concerning the bond stress versus the relative slip; and (d) comparison of FEM results with the tests by Shima et al. (1987c).

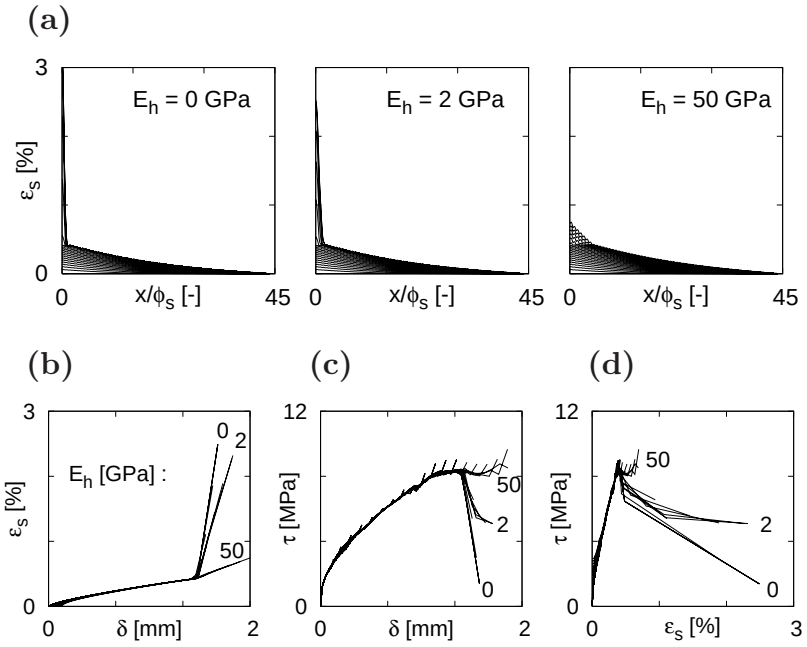

Fig. 9 - FEM results with the geometry and properties of specimen SD–70 (Shima et al., 1987a), for different hardening moduli of the bar (E_h): (a) strain profiles; and (b) various diagrams (bar strain and bond stress versus bar slip, and bond stress versus bar strain) for all load steps and bar sections.

10, where a rather satisfactory agreement is achieved for the three cases and a similar shape of the post–yield branch is observed for the different specimens.

The similarity in the descending branches (Fig.10d) confirms that adopting a bond coefficient to correct the local bond-slip law in the post-yield phase of a bar (see Fernández Ruiz et al., 2007) is sound, as will be shown later.

5.4 Radial strains

A reinforcing bar undergoes a lateral expansion/contraction when it is loaded, both in the elastic domain (controlled by the Poisson's coefficient ν_e) and in the plastic domain (where the volume of the bar remains constant according to Von Mises' yield criterion for steel).

The influence of this phenomenon has been studied by means of finite elements, with the geometry and properties of the previously-described specimen SD–70. The elastic and plastic responses of bond have been analyzed under different situations concerning the lateral strain in the bar.

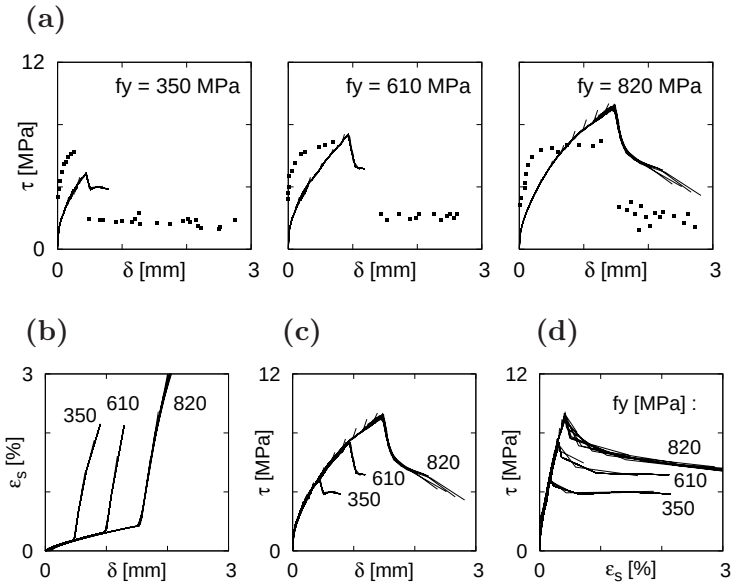

Fig. 10 - Influence of the yield strength in the post–yield response of bond: (a) comparison of FEM results with the tests by Shima et al. (1987a); and (b) numerical results (bar strain and bond stress versus bar slip, and bond stress versus bar strain).

The influence of Poisson's coefficient seems to be somewhat limited as shown in Fig.11a for various values of ν_e. In any case, larger bond stresses in the elastic domain of the bar are obtained when ν_e is small or zero (because of the smaller lateral contraction of the bar). However, once the bar yields, the tendency of the volume to remain constant becomes the determinant factor and the role of Poisson's coefficient becomes negligible.

Figure 11c shows the results of a numerical test where the radial displacements of the reinforcing bar have been blocked at the interface with the concrete, as sketched in Fig.11b. In this case, even in the post–yield domain of the steel, the bond stresses increase because the bar undergoes no lateral contraction (in accordance with the results obtained in push–in tests). This response allows to identify the lateral contraction of the bar in the plastic domain as one of the main parameters controlling the post–yield behavior of bond.

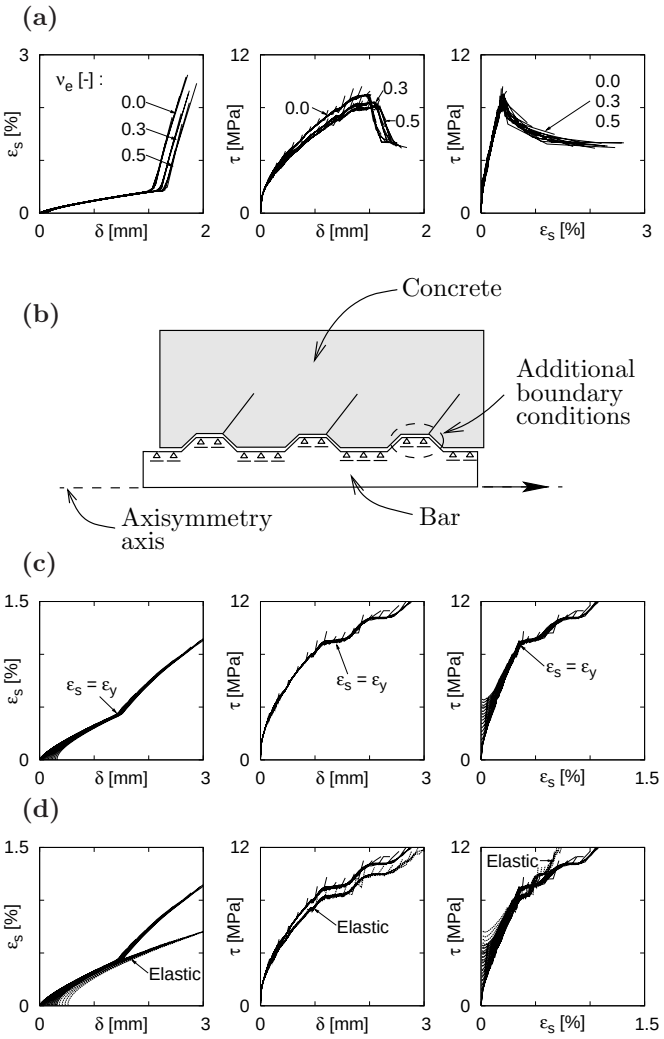

Fig. 11 - Influence of the lateral contraction of the bar on bond response in pull-out tests : (a) various diagrams (bar strain and bond stress versus bar slip, and bond stress versus bar strain) obtained with FE analysis, for different values of the Poisson's coefficient; (b) details concerning the additional restraints introduced into the analysis to prevent bar contraction; (c) various diagrams with fully-prevented lateral contraction (laterally-restrained bar); and (d) comparison between the elastic-plastic laterally-restrained bar (top in left and middle figures, and bottom in right figure) and a fully-elastic laterally-free bar.

Finally, in Fig.11d a comparison is made between the case of the elastic-plastic laterally-restrained bar (EPLR, as in Fig.11c) and that of a fully-elastic laterally-free bar (FELF). The middle figure shows that the difference between EPLR (top) and FELF (bottom) is very limited, this being a demonstration that the lateral strain has little effect on bond, as long as the bar is in the elastic domain.

5.5 Local influence of previous parameters on bond stresses

The previous analyses demonstrate that several phenomena (strain hardening, lateral contraction/expansion of the bar ...) affect the local response of bond in embedded bars, where two regimes (before and after bar yielding) occur.

The post–yield behavior of bond is greatly influenced by the radial strains in the bar that lead to sizable differences in the response of the members subjected to pull-out and of those subjected to push-in. In order to introduce this phenomenon in the local response of bond, the bond stress should be in some way corrected, whenever the effects of the lateral strains cannot be neglected, by multiplying τ_s by a bond coefficient K_b (≤ 1). For this coefficient a formulation is proposed in the following as a function of the longitudinal strain in the bar, since the lateral strain is directly related to the longitudinal strain:

$$\tau = K_b(\varepsilon_s/\ \varepsilon_y) \cdot \tau_s$$

where τ_s is the local stress equal to the mean stress in the pull-out test of a short anchored bar.

The coefficient K_b can be computed for any given configuration to take into account the influence of the various properties of the bar, of the concrete and of their interface. As previously seen, the influence of the lateral strain on bond response is limited in the elastic domain of the bar (for both short- and long-embedment lengths). Consequently, in these cases K_b should be equal to unity ($\tau = \tau_s$).

Figure 12b shows for instance the values of the bond coefficient K_b in the reinforcing bars having different yield strengths (same values for f_y as in Fig.10). It can be seen that –regardless of the yield strength– all curves follow a similar pattern.

A general formulation of the bond coefficient, valid for any reinforcing bar, as well as an application of this coefficient in the analytical modeling of bond in reinforced concrete is further discussed in Fernández Ruiz et al. (2007).

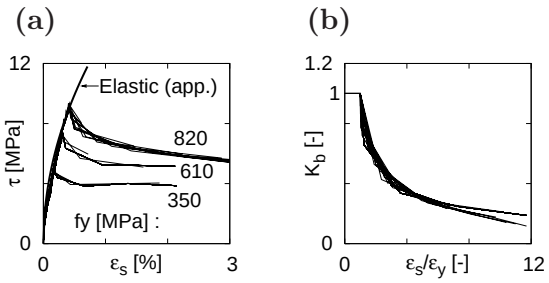

Fig. 12 - Bond coefficient (K_b): (a) numerical results concerning the bond stress as a function of the relative slip for different yield-strength values (elastic response); and (b) computed values of the bond coefficient for the 3 values of the yield strength of the steel introduced in Fig.10.

6. TENSION TIES

Tension ties are reinforced–concrete specimens that represent the concrete prism limited by two contiguous flexural cracks and reinforced by a bar pulled at both ends. In the literature, numerous results can be found on both tension ties (concrete cylinders reinforced with a single bar, see Engström, 1992; and Kankam, 1997) and reinforced beams subjected to pure bending (Kenel, 2002; and Harajli, 2004; Laurencet, 1999).

6.1 Elastic behavior of the reinforcing bar

Kankam (1997) performed several tensile tests on short R/C ties. Figure 13 shows the distribution of the strains measured by Kankam on a 25–mm cold–worked ribbed bar for different load levels. Though FEM results are more than satisfactory, some differences appear in the response at very-low strain values. One explanation may be that the model does not consider concrete softening in tension along the inner inclined cracks, but it is doubtful whether at low strain levels there are any sizable inclined cracks.

6.2 Elastic–plastic behavior of the reinforcing bar

Five reinforced- and prestressed–concrete beams were tested by Kenel and Marti (2001), who measured the strains in the reinforcement, by means of Bragg grating sensors, before and after bar yielding. In FE modeling, the stress distribution in the tensile reinforcement (top bars in Fig.14a) is assumed to be uniform, and the tensile stresses in the concrete between two contiguous flexural cracks and along the crack faces are assumed to be zero.

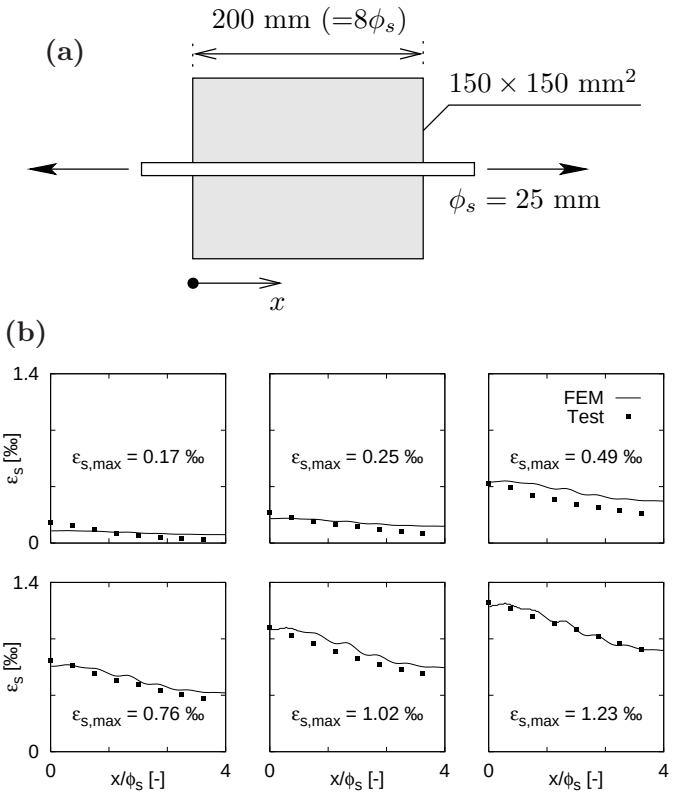

Fig. 13 - Tests by Kankam (1997): (a) test set–up (E_s = 200 GPa, concrete cylindrical strength f_c = 42 MPa); and (b) fitting of test results for different load levels.

Figure 14 (b) shows a satisfactory agreement between testing and modeling, in terms of steel strains as a function of the section coordinate. In Fig.14c the bond stress is plotted as a function of both the slip and the steel strain, the latter being in turn plotted as a function of the former. In each picture of Fig.14c, there are 3 curves, each of them referring to a specific section of the specimen, starting from the plane containing a flexural crack. Sections A and B are one and two rib-spacing apart, while Section C is three or more rib-spacing apart. While the curves $\tau(\delta)$, $\tau(\varepsilon_s)$ and $\varepsilon_s(\delta)$ of Sections B and C tend to coincide (or are very close), the curves of Section A denote a marked decay of bond performance.

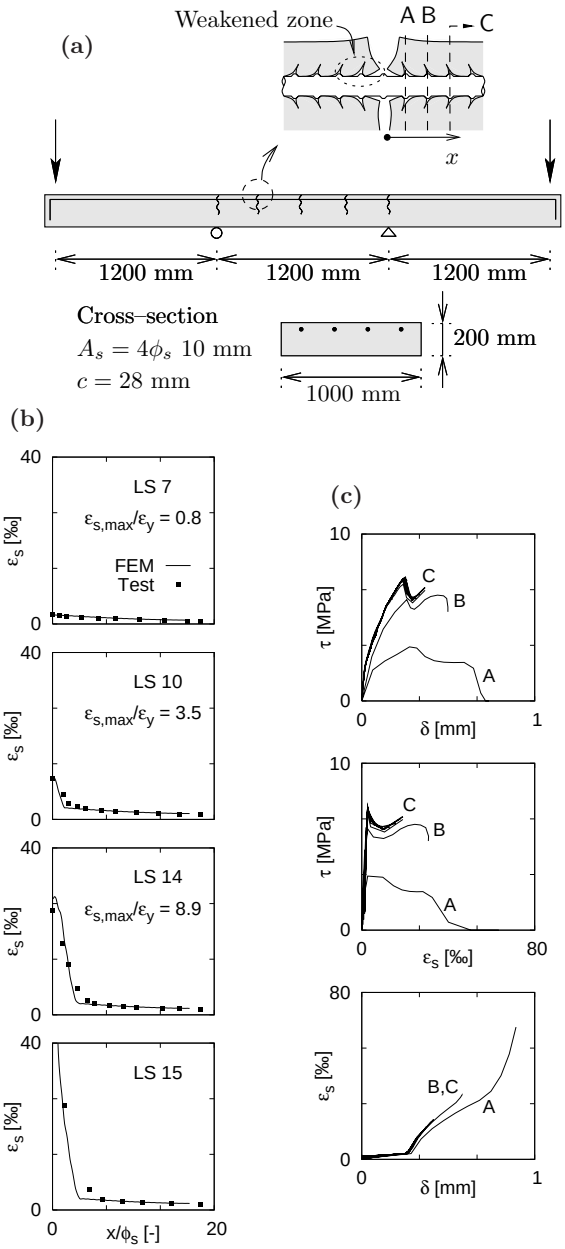

Fig. 14 - Test on Beam B4 (E_s = 208 GPa, f_y = 584 MPa, E_h = 2.8 GPa, f_c = 37 MPa) by Kenel and Marti (2001): (a) test set–up (sections A and B defined by the ribs closest to the flexural cracks, and C representing any other section containing a rib); (b) FE analysis and test results concerning the steel strain profiles at different load levels (max. strain in the reinforcement not available for the last load step); and (c) various plots of the numerical results. LS = Load Step.

The reason of this difference is the development of conical microcracks close to the flexural cracks (see Fig.14a), that weaken bond response close to the flexural cracks, because of the local punching of the concrete. In this case, the local bond stress–slip law should be corrected, as already mentioned. This effect – that depends on the rib shape and on the load level of the bar (since the larger the load, the more extended the inclined microcracks) – agrees with the bond reduction factor for tension ties introduced by Fernández Ruiz et al. (2007).

7. CONCLUSIONS

Bond mechanics is modeled in this paper by means of finite elements, in order to study various bond–related problems, that have been so far hardly or little investigated for a number of objective experimental difficulties. The agreement with the test data (whenever available) is satisfactory, and the cross-examination of the numerical and experimental results leads to the following main findings with reference to both bond response and failure modes:

1. Finite-element analysis confirms the uniqueness of the bond stress–slip law for short and long anchored bars, on condition that the section considered is at least 3 or more rib-spacing apart from any through crack (due to bending in beams or to tensile forces in tension ties).
2. A unique steel strain–slip relationship can be worked out, this being a demonstration of the validity of the affinity hypothesis proposed by Fernández Ruiz et al. (2007).
3. Bar yielding marks the threshold between two different regimes, with sizable consequences on the relationships between the bond stress, the bar slip and the steel strain.
4. For tension bars in cracked concrete, finite elements confirm that bond is weaker close to the through cracks due to the formation of local cone–shaped microcracks ("punching" microcracks). The influence of these microcracks depends on the load level and on the size of the member, but is limited to a distance – from any through crack - close to 3 times the rib spacing. This result is in agreement with the bond reduction factor proposed in Fernández Ruiz et al. (2007).
5. The main parameters controlling bond response before bar yielding (provided that concrete cover prevents any concrete splitting) are rib geometry, concrete strength and bar stiffness (elastic modulus), while the influence of Poisson's ratio in this phase is rather limited.
6. Concerning the post–yield response of an anchored bar, the hardening modulus of the steel seems to be the main parameter controlling bond

behavior, whereas other parameters – such as the strength at yielding – have a rather limited influence.

7. The post–yield response of bond is influenced by the radial strains in the bar. The occurrence of these strains explains why in the pull–out mode the behavior of long specimens markedly differs from that in the push–in mode. With regard to this point, the role of the radial strains has been investigated by performing a few analyses with fully–blocked radial displacements at the bar–concrete interface: the lack of lateral contraction makes the behavior of the yielded bar very close to that of an elastic bar, in terms of bond–stress distribution. This is a demonstration of the major role played by bar lateral contraction in the post-yield phase.
8. Bond modeling in the post–yield phase can be performed by introducing a "bond coefficient" taking into account the hardening modulus and the longitudinal strain in the bar (in this way, the effects of the radial strain are properly considered, since this strain is directly related to the longitudinal strain). The bond coefficient is constant, and has a unit value, as long as the local bar strain remains below the yield threshold, while decreases sharply above the yield threshold. Consequently, in the pull–out tests of plasticized bars the bond strength – and more generally – the bond-stress/slip law exhibit reduced values, compared to the elastic case.

Notation

E_s , E_h = elastic and hardening moduli of the steel
F = force
K_b = bond coefficient
L = bonded length
c = concrete cover
f_c = concrete cylindrical compressive strength (wherever necessary, the cylindrical-to-cubic strength ratio is assumed to be 0.83)
f_y = steel strength at yielding
δ = relative bar–concrete slip
ε_s , ε_y = strain in a rebar ; steel strain at yielding
ν_e = Poisson's coefficient
ϕ_s = bar diameter
λ = local punching coefficient
σ_s = stress in a steel bar
σ_i = principal stresses (i=1, 2, 3)
τ = local bond stress (at any point of a bar)
τ_s = bond stress in a short anchored bar (almost constant for $L/\phi_s \leq 5$)
τ_{max} = maximum bond stress

REFERENCES

Bamonte P.F., Coronelli D. and Gambarova P.G. (2003). "Smooth Anchored Bars in NSC and HPC: A Study on Size Effect". *Japan Concrete Institute - Journal of Advanced Concrete Technology*, Vol. 1, No. 1, pp. 42-53.

Bamonte P.F. and Gambarova P.G. (2007). "High-Bond Bars in NSC and HPC: Study on Size Effect and on Local Bond Stress-Slip Law". *ASCE - Journal of Structural Engineering*, Vol.113, No. 2, pp. 225-234.

Bigaj A.J. (1995). *Bond Behaviour of Deformed Bars in NSC and HSC. Experimental Study*. Faculty of Civil Engineering, Delft University of Technology, Report 25.5–95–II, Delft, The Netherlands, 132 pp.

Bigaj A.J. (1999). *Structural Dependence of Rotation Capacity of Plastic Hinges in RC Beams and Slabs*. PhD Thesis, Faculty of Civil Engineering, Delft University of Technology, Delft, The Netherlands, 230 pp.

Engström B. (1992). *Ductility of Tie Connections in Precast Structures*. PhD Thesis, Chalmers University of Technology, Göteborg, Sweden, 368 pp.

Fernández Ruiz M., Muttoni A. and Gambarova P.G. (2007). "Analytical Model on the Pre- and Post–Yield Behavior of Bond in Structural Concrete". *ASCE - Journal of Structural Engineering*, to be published in October 2007.

Fédération Internationale du Béton – FIB (2000). *Bond of Reinforcement in Concrete*. Bulletin No. 10, State-of-Art Report T.G. 4/2 Bond Models, FIB, Lausanne, Switzerland, 427 pp.

Harajli M.H. (2004). "Comparison of Bond Strength of Steel Bars in Normal and High–Strength Concrete". *ASCE - Journal of Materials in Civil Engineering*, Vol. 16, No. 4, pp. 365–374.

Kankam C. K. (1997). "Relationship of Bond Stress, Steel Stress and Slip in Reinforced Concrete". *ASCE - Journal of Structural Engineering*, Vol. 123, No. 1, pp. 79–85.

Kenel A. and Marti P. (2001). *Optic–Fibre Strain Measurements in Embedded Reinforcing Bars* (in German), ETHZ - Swiss Federal Institute of Technology at Zurich, Birkhäuser, Basel-Boston-Berlin Zürich, Report No. 271, Zurich, Switzerland, 93 pp.

Kenel A. (2002). *Flexural Behaviour and Minimal Reinforcement in Reinforced-Concrete Structural Elements* (in German), ETHZ - Swiss Federal Institute of Technology at Zurich, PhD Thesis 14874, Zurich, Switzerland, 115 pp.

Laurencet P. (1999). *Prestressing and Minimal Reinforcement for the Control of the Residual Crack Width* (in French), EPFL - Swiss Federal Institute of Technology at Lausanne, PhD Thesis 2028, Lausanne, Switzerland, 258 pp.

Lundgren K. (2001). “Three-Dimensional Modeling of Anchorage Zones In Reinforced Concrete”, *ASCE - Journal of Engineering Mechanics*, Vol. 127, No. 7, pp. 693–699.

Ngo D. and Scordelis A. C. (1967). “Finite-Element Analysis of Reinforced-Concrete Beams”. *ACI Journal*, Vol.64, No.3, pp.152–163.

Russo G. and Romano F. (1991). “Bond Response in a Push–In / Pull–Out Test when the Rebar and the Concrete are Loaded at Opposite Ends”. *Studi e Ricerche*, Vol.12, Politecnico di Milano/Milan University of Technology, Milan, Italy, pp. 19–44.

Salem H. M. and Maekawa K. (2004). “Pre– and Post-Yield Finite-Element Method Simulation of Bond of Ribbed Reinforcing Bars”. *ASCE - Journal of Structural Engineering*, Vol. 130, No. 4, pp. 671–680.

Schenkel M. (1998). *On Bond Behaviour of Reinforcing Bars with Limited Cover* (in German). ETHZ - Swiss Federal Institute of Technology at Zurich, Birkhäuser, Basel-Boston-Berlin, Report No. 237, Switzerland, 162 pp.

Shima, H., Chou, L–L. and Okamura, H. (1987a) “Bond Characteristics in Post–Yield Range of Deformed Bars”, *Concrete Library of JSCE (Translation from the Proceedings of the Japan Society of Civil Engineers*, *No. 378/V-6)*, No. 10, pp.113–124.

Shima H., Chou L–L and Okamura H. (1987b). “Micro- and Macro-Models for Bond in Reinforced Concrete”. *Journal of the School of Engineering*, University of Tokyo, Vol. XXXIX, No 2, pp.133–194.

Shima H., Chou L–L and Okamura H. (1987c). “Bond–Slip–Strain Relationship of Deformed Bars Embedded in Massive Concrete”. *Concrete Library of JSCE (Translation from the Proceedings of JSCE, No 378/V-6)*, No. 10, pp. 79–94.